MM Science Journal | www.mmscience.eu
ISSN 1803-1269 (Print) | ISSN 1805-0476 (Online)
Special Issue | HSM 2023
17th International Conference on High Speed Machining
October 25-28, 2023, Nanjing, China
DOI: 10.17973/MMSJ.2023_11_2023105

HSM2023-00014

# FUNDAMENTAL ANALYSIS ON THE DYNAMIC BEHAVIOR OF TOOLS WITH STRUCTURED FUNCTIONAL SURFACES IN CUTTING OPERATIONS

S. Jaquet[1]*, J. Baumann[1], R. Garcia[1], D. Biermann[1]
[1]TU Dortmund University, Institute of Machining Technology (ISF), Dortmund, Germany
*Corresponding author; e-mail: simon.jaquet@tu-dortmund.de

**Abstract**

The productivity of machining processes is often limited by the occurrence of dynamic effects. The investigated approach intends to counteract tool deflections, and thus to damp and disrupt chatter vibrations by using milling tools with defined functional structures on the flank faces at the frontal cutting edges. For the fundamental investigation of the interactions between structural geometric properties and the tool-workpiece interaction, the engagement situation was geometrically evaluated on a highly abstracted level. Subsequently, hypotheses derived from this were validated experimentally in analogy tests with linear cutting motion. In these cutting experiments, dynamic deflections were induced by an external excitation of the specifically compliant modular tool system. Finally, the technologically most relevant structure variants were applied to milling tools and evaluated with regard to their dynamic behavior. This investigation was preceded by a simulation-based analysis of the material removal on the frontal flank face as a function of the process configuration, which is characterized by multiple intersecting cuts in milling processes. By specifically optimizing and coordinating the structure design and the process configuration, an increase in process stability and thus productivity of at least 100% could be achieved.

**Keywords:**
Cutting tools, Chatter avoidance, Surface structures

## 1 INTRODUCTION

The efficient design of cutting processes is limited by the maximum material removal rates (MRR) to be achieved, considering the desired accuracy at minimal costs. Such goals could be achieved by high feed rates and tool engagement [Denkena 2011, Denkena 2016]. By maximizing these parameters, unwanted disturbance effects can occur, such as high thermal loads, static displacement as well as dynamic effects like chatter [Dietrich 2016]. With the development of new cutting materials in machining, the realization of high MRR has become possible. Due to these possibilities, in addition to the higher nominal power of newer machines, the risk of vibrations in the machining process has strongly increased. This requires the development of new methods for process stabilization [Munoa 2016]. Chatter in the sense of a self-excited vibration depends on many factors. Examples are the dynamic stiffness, the geometry of the tool, as well as process parameters such as the cutting speed or the feed per tooth [Munoa 2016]. The suppression of dynamic effects constitutes a significant challenge although various approaches have been developed. The investigated approach is intended to increase process damping and disrupt the regenerative effect based on structuring the flank face of the frontal cutting edge (Fig. 1).

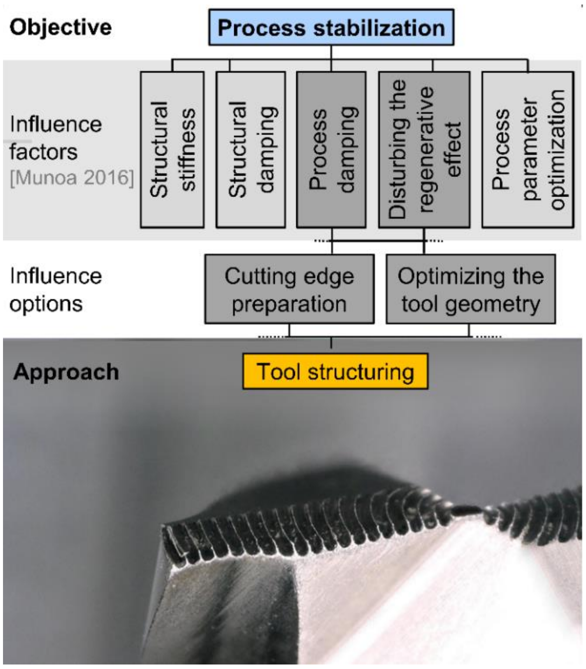


*Fig. 1: Potential process stabilization approaches [Baumann 19].*

It can be concluded that a variety of process stabilization options exist, which can be divided into five options. Enhancing the structural stiffness and damping, the process parameter value selection, the process damping maximization, and the regeneration disturbance. Increasing the structural stiffness or damping of machine tools constitutes a challenge in engineering, as it is associated with high costs and restricted in terms of scalability [Hirsch 2012, Munoa 2016, Möhring 2017, Vogel 2018]. An optimized process parameter value selection requires a detailed determination of the dynamic properties of the production system [Altintas 2014, Munoa 2016]. Maximizing process damping [Sellmeier 2012, Munoa 2016] and disturbing the regenerative effect [Denkena 2010, Sellmeier 2012] is largely independent of the properties of the production system and process, which is why these methods are particularly interesting in the sense of a universally applicable strategy for increasing productivity.

In previous work it was shown that by modifying and structuring the frontal cutting edge of a milling tool, the process stability can be increased [Baumann 2019]. However, the effect of the process design on the cutting kinematics was not specified in detail. Therefore, the aim of this work is to analyze these mechanisms of action in more detail and to provide a target design of the microscopic structures. In particular, a correlation between the shape of the structure and the stabilization potential is investigated.

## 2 WORKING HYPOTHESIS

According to the derived working hypothesis the microstructure inhibits tool vibration by an increase in contact forces. The microscopic structure of the tools interacts with the workpiece material to increase damping potential and counteract the radial dynamic deflection as depicted in Fig. 2. The applied structure increases the contact surface on the tool and provide surface sections with normal alignment to the deflection, which enables support and guidance of the tool within its motion of cut. Plastic deformation and friction effects may also absorb energy, and thus damp dynamic deflections.

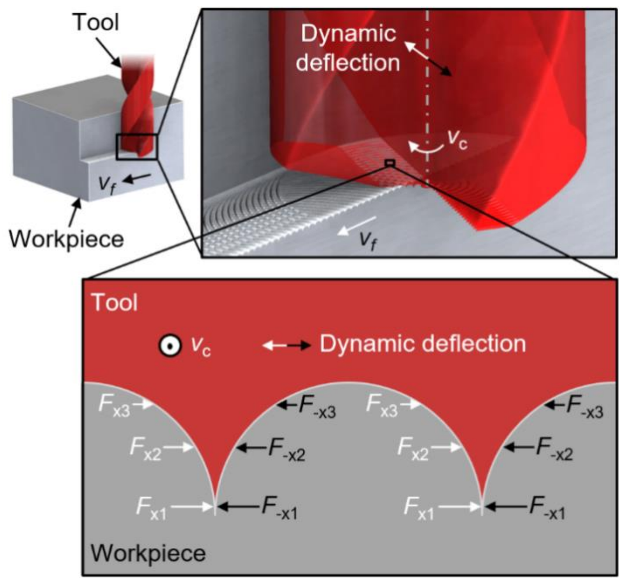


*Fig. 2: Illustration of the working hypothesis [Baumann 19].*

## 3 GEOMETRIC ANALYSIS

For the fundamental investigation of the interactions between structural geometric properties and the tool-workpiece interaction, the engagement situation was geometrically evaluated on a highly abstracted, two-dimensional level.

### 3.1 Microstructure shape

Microstructuring allows structures of different structural shapes to be produced. However, the applied production process limits the degrees of freedom. The reference point were the arc-shaped structures described in [Baumann 2019]. The initial analysis consisted of the identification of the geometric degrees of freedom, under the condition of manufacturability. For instance, the depth $d_s$, the width $w_s$, and the radius of the arc $r_s$ can be varied (Fig. 3). Subsequently, the effect of different structure shapes on the stabilization potential was investigated. It was necessary to consider the possibilities available regarding microscopic structuring, since these represent specific boundary conditions with regard to the scope for design. Triangular structures were found to be a viable alternative to arc-shaped structures. These provide a resultant force vector oriented similar to a semi-circular structure and thus, should accommodate tangential forces due to vibration of the tool. Moreover, this structure shape is machineable by micro milling with tilted end mills. Other shapes, such as sinusoidal or rectangular structures, are likewise conceivable.

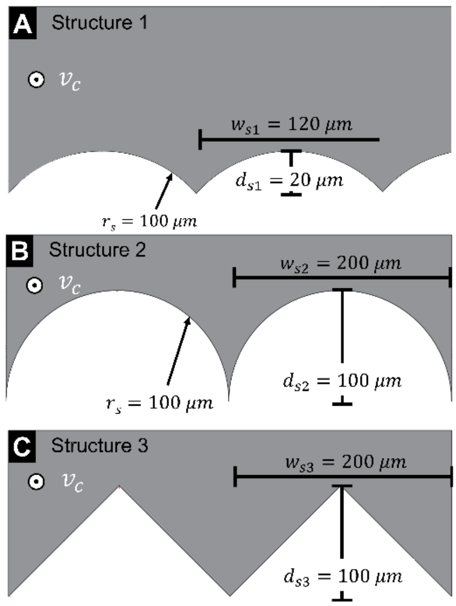


*Fig. 3: Geometry of the observed structure variants.*

### 3.2 Tool workpiece Interaction

The idea of microscopic structuring on the flank face consists of the interaction between the tool and the material and the resulting absorption of lateral forces, as they occur during chatter vibration. In an orthogonal cut, all microstructure elements are aligned parallel. However, in the milling process, depending on the feed per tooth, there are many feed steps until structure elements near the tool center point (TCP) come into interaction with the material.

Therefore, feed steps were included in the geometric consideration (Fig. 4). The width of engagement was increased by the feed step $f_s$ after each linear cutting motion (analogy feed per tooth). This leads to correlations between the structural shape and the feed steps, which need to be characterized in more detail.

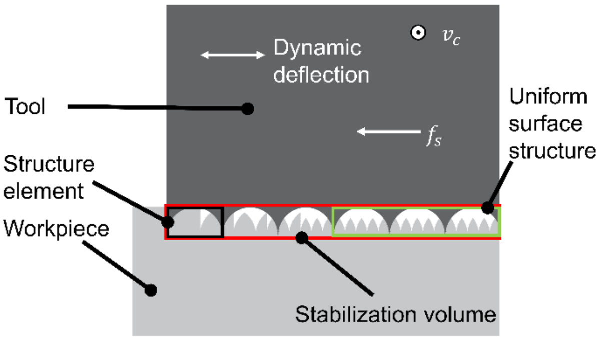


*Fig. 4 Geometry of the Tool-workpiece interaction.*

The interaction of the microstructure with the workpiece in the effective zone was investigated. The material removal as a function of the structure and the feed steps was defined as an influencing factor. The underlying hypothesis was that the "potential stabilization volume" (PSV), which remains under the microstructure, can still interact with following structure elements and thus contribute to stabilizing the process. This consideration is highly simplified compared to the milling process, where the rotatory cutting and superimposed translatory feed motion of the tool creates a much more complex surface structure. Above a certain number of feed steps, no additional PSV is removed, and a uniform surface structure is formed on the component as following structure elements only move through pre-cut groves.

The influence of the feed steps and the structural shape on the PSV was examined in more detail. For this purpose, a fictitious workpiece with dimensions in height(H) x width(W) x length(L) of 10x3x1 mm³ was constructed. The tool dimensions were defined as 10x5x1 mm³ in height(H) x width(W) x length(L). Both the already known arc-shaped structures and a triangle-shaped structure with a structure depth $d_s$ = 100 µm were analyzed (Fig. 5). As depicted and expected, the deepest arc-shaped structure leads to the largest increase in PSV. In theory, therefore, the elements following the initial intersecting structural element should remove a large $V_{PSV}$ and thus strongly contribute to the guidance of the tool by absorbing the dynamic transverse forces. In general, it can be stated that the deeper the arc-shaped structure, the greater the stabilization volume. Due to the generally lower PSV-level when triangular structures are modeled, this approach was discarded in the following. The same reasoning applies to other conceivable structures (e.g., rectangular and undulating shapes).

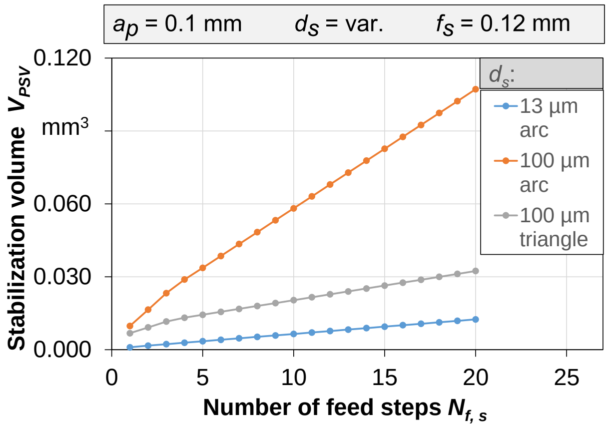


*Fig. 5 Potential stabilization volume in dependency of the number of feed steps.*

## 4 ANALOGY TESTS WITH LINEAR CUTTING MOTION

Subsequently, hypotheses derived from this were validated experimentally in analogy tests with a linear cutting motion. The use of various actuating and measurement systems allowed a comprehensive process analysis.

### 4.1 Test setup

In these cutting experiments, dynamic deflections were induced by an external excitation of the specifically compliant modular tool system presented in [Woeste 2020]. Thus, a dynamically controlled experimental setup was established (Fig. 6).

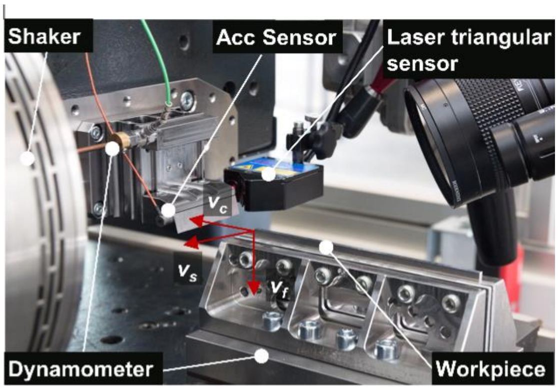


*Fig. 6: Test setup for the analogy tests.*

### 4.2 Tool preparation

High-speed steel (HSS) blanks of AISI M2 formed the basis for the cutting tools. These were quenched and tempered using the manufacturing process described in [Woeste 2021] to produce a martensitic microstructure. The blanks were modified in the area of the cutting edge. A rake and clearance angle of 10° each was applied by grinding to produce a defined cutting edge (Fig. 7).

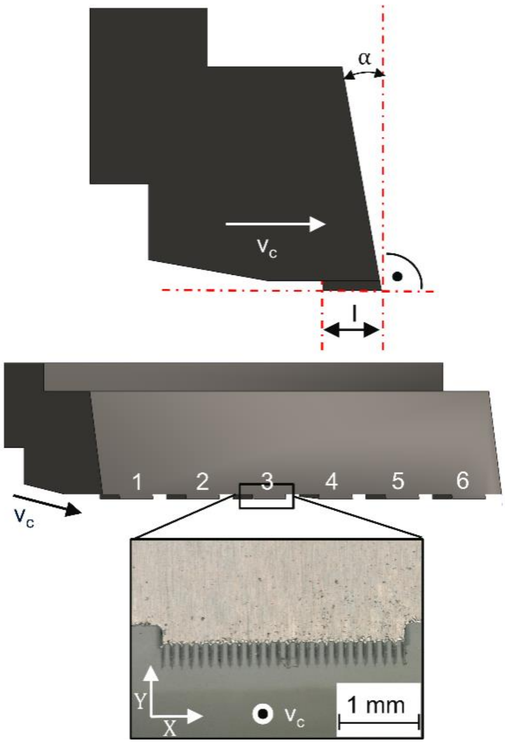


*Fig. 7: Cutting element and tool preparation.*

Further processing was executed in micro milling processes. First, a flank face chamfer with a clearance angle of 0° was applied. To ensure a constant length of the clearance chamfer, a notch was prepared in a distance of $l_s$ to the cutting edge. This ensured a defined structure length $l_s$, regardless of their structure depth. Micro milling performed the micro structuring. The structures were produced using a ball cutter with $r_s$ = 100 µm. To prevent frequent reclamping of the cutting elements on the machine, several variations of structures were applied on one cutting element. The microstructures were varied on surfaces 1, 2, 3, 5 and 6. Cutting edge 4 only served as a reference with a rake and clearance angle of 10° each. The structure applied to the flank face of the cutting element was varied in terms of its depth. The shape used was restricted to the arc-shaped structure. The structure depth and the structure width were varied, with a constant structure radius of $r_s$ = 100 µm.

*Tab. 1: Prepared tool variants.*

| Tool | Structure depth in µm | Structure width in µm | Arc radius in µm |
|---|---|---|---|
| 1 | 100 | 200 | 100 |
| 2 | 69 | 190 | 100 |
| 3 | 56 | 180 | 100 |
| 5 | 40 | 160 | 100 |
| 6 | 34 | 150 | 100 |
| 7 | 29 | 140 | 100 |
| 8 | 13 | 100 | 100 |

### 4.3 Results

An exemplary process force progression is depicted in Fig. 8. In this experiment a modified flank face chamfer with the structure depth $d_s$ = 13 µm was used. The cutting speed was set to $v_c$ = 120 m/min at a cutting depth of $a_p$ = 0.1 mm. The tool was excited externally in the tangential cutting direction at a frequency of $f_{ex}$ = 1200 Hz. The cutting force $F_c$ approaches 445 N, which is about 57 % less than the normal force $F_N$ = 1045 N. The tangential force $F_t$ oscillates around the zero-position due to the sinusoidal excitation. Within tool engagement, a tangential force transmission is executed in the direction of the excitation, which indicates the absorption of dynamic lateral forces. In the further evaluation of the tangential force, the periodic excitation is referred to the force magnitude defined as $F_{t,O}$. The evaluation of the cutting force $F_c$ and normal force $F_n$ refers to the mean level.

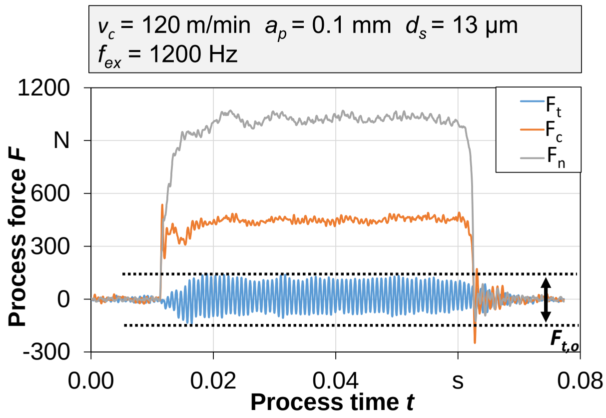


*Fig. 8: Force progression during one cut of the analogy tests.*

A closer look at the force measurements also reveals a slight oscillation of the cutting force and normal force around their mean values. To classify the oscillation more precisely, the autospectrum of the cutting force is depicted in Fig. 9. At the excitation frequency of $f_{ex}$ = 1200 Hz, a dominant force amplitude in the cutting direction can be identified. In addition, an increased amplitude in the range of the dominant natural frequency at $f_0$ = 1550 Hz is evident.

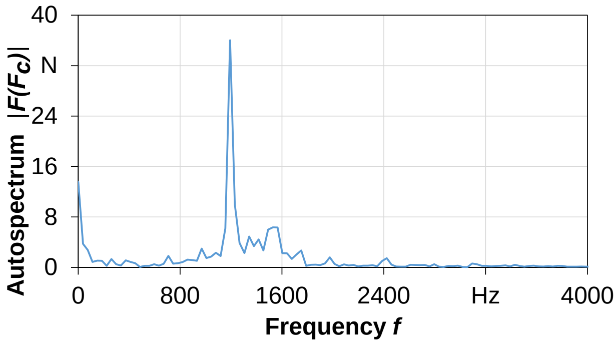


*Fig. 9: Autospectrum of the cutting force component $F_c$.*

The measured acceleration at the cutting element is provided in Fig. 10 for an experiment using a structured flank face. With respect to the acceleration, the sinusoidal excitation provided by the electromagnetic shaker can first be observed in free oscillation. When the cutting element engages into the specimen at about $t_e$ = 0.012 s the acceleration amplitude decreases from 412 m/s² to 344 m/s². This observation indicates, that the structure-based tool modification not only allows the transmission of lateral forces, but also provides a damping of periodic deflections. At the end of engagement, a post-oscillation of the tool can be observed.

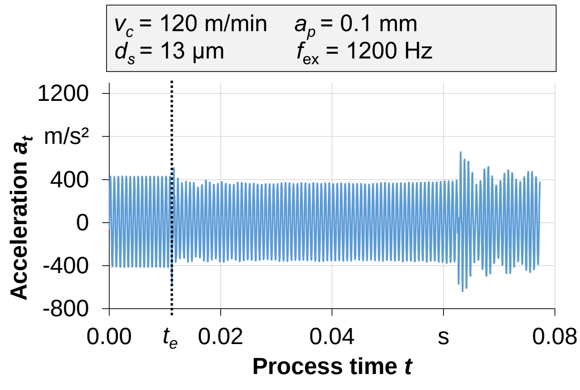


*Fig. 10: Acceleration in direction of dynamic excitation.*

The dynamic component of the tangential force $F_{t,\,O}$ represents one of the decisive parameters of the stabilization potential, since it counteracts the force applied by the dynamic deflection. In the following, this force is defined as stabilization force $F_{t,\,O}$. In Fig. 11, this force $F_{t,\,O}$ is compared to the reference tool for different structure depths $d_s$. The reference tool is defined as $d_s$ = 0 µm, the flat flank face chamfer as $d_s$ = 1 µm. An initial increase in the transmitted force is observed. The determined force for the flat flank face chamfer is 56.6 N. This increases in the case of $d_s$ = 13 µm to a value of 97.6 N and reaches its maximum value of 119.1 N for the deepest structure with $d_s$ =100 µm. The transmitted force thereby increases with the structure depth as derived geometrically. It can be assumed that a modification of the flank face chamfer enables a significant stabilization potential.

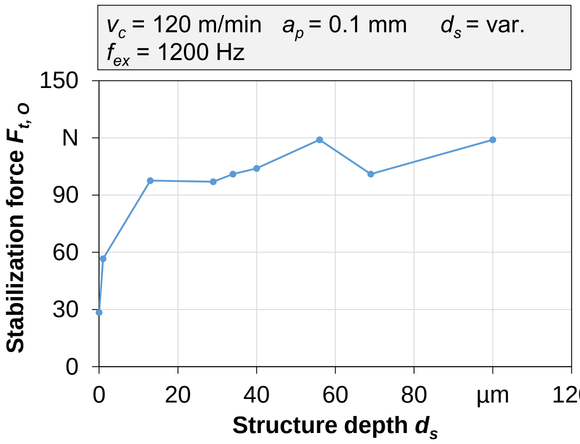


Fig. 11: Measured dynamic part of tangential force.

In terms of the force counteracting the dynamic excitation and oscillation, it can be stated that with an arc-shaped structure with a depth of $d_s$ = 100 µm, compared with the reference tool the force $F_{t,\,O}$ is higher by a factor of about 4.

To increase the analogy of the cutting operation with a linear cutting motion to the milling process, a feed step $f_s$ was introduced. This was defined in the direction of $a_e$ at constant $a_p$ and represented the analogy to the feed per tooth in milling. The feed step kept constant at $f_s$ = 0.12 mm and the structure depths $d_s$ were varied. The depth of cut was constant $a_p$ = 100 µm and the excitation frequency was 1200 Hz. Fig. 12 depicts the normal force $F_n$ as a function of the number of feed steps for different arc depths. The arc depth $d_s$ = 1 µm defines the tool with a non-structured, flat chamfer again. It can be stated that the reference tool has an almost constant force level of 10-15 N through all feed steps. For the modified flanks, the normal force increases with increasing $a_e$. After 20 feed steps, the tool with flank chamfer has the highest normal force of 541 N. With increasing structure depth and the resulting shift of the force application vector, the normal force decreases. After 20 feed steps, this amounts to 368 N for a structure depth of $d_s$ = 100 µm.

However, relevant for the transfer of the results from cutting operation with a linear cutting motion to the milling process, are the stabilization forces in dependence of the number of feed steps, which counteract the deflection of the tool during periodic excitation. The stabilization force is compared against the reference tool in Fig. 13 depending on the number of feed steps to a modified tool with an structure depth of $d_s$ = 34 µm.

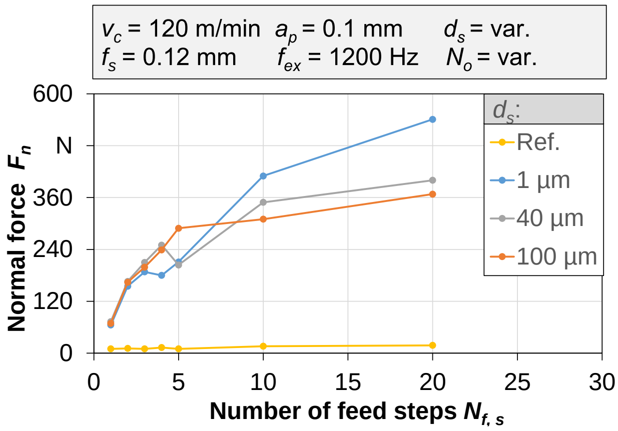


Fig. 12: Measured normal force $F_n$ with respect to number of feed steps.

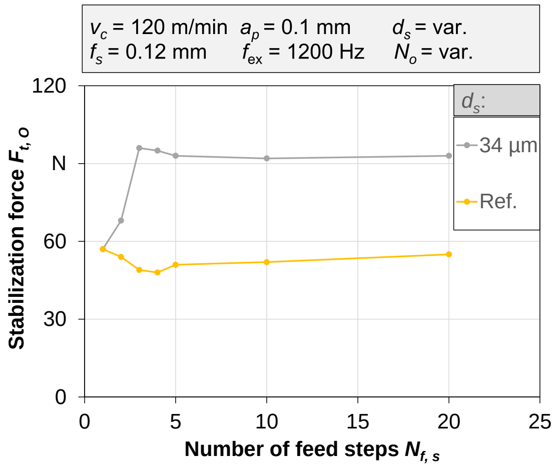


Fig. 13: Measured dynamic part of the tangential force with respect to number of feed steps.

The modified tool reaches its maximum force after three feed steps and then approaches a constant level. The increase cannot be observed when using the reference tool and a constant force is transmitted.

## 5 GEOMETRIC PHYSICALLY-BASED MILLING SIMULATION

In the previous chapters, it was verified that the PSV between tool and workpiece is a relevant criterion for the stabilization potential. This analogy was considered in more detail for the milling process. The modification of the cutting tool models was realized on the frontal cutting edges. The milling process has a crucial difference compared to the analogy tests. Firstly, a much more complex surface structure is created in the milling process due to the superposition of the translational and rotational motion. Secondly, the milling tool has a multidimensional oscillation orbit, compared to the one-dimensional oscillation in the analogy experiment. The analogy of the milling process to the orthogonal cutting would be the oscillation of the tool in the direction of the feed vector in the case $a_e$ equal to the tool radius. However, the oscillation orbit deviates from this representation and was simulated for an exemplary milling process. A two-fluted milling tool with diameter $d$ = 8 mm and cantilever length of 35 mm was assumed. The process data can be taken from the Fig. 14. Under the defined process conditions, the tool has a two-dimensional orbit, which is shifted in its principal direction of oscillation by an angle $\alpha$ to the feed direction.

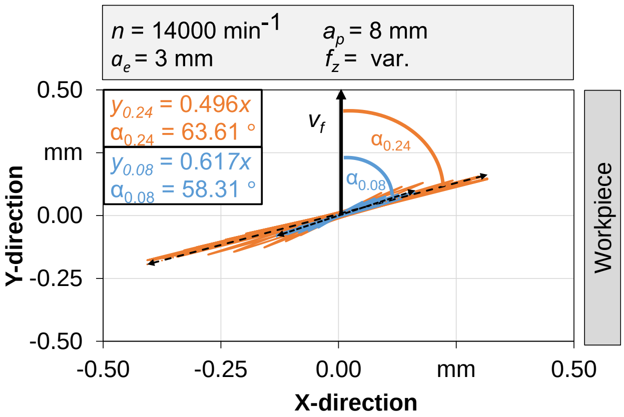


*Fig. 14: Tool center point orbit.*

This is a function of the underlying process parameters and modal properties of the system. The deflection is shown exemplarily for two different feed per tooth $f_z = 0.08$ mm and $f_z = 0.24$ mm.

In the previous chapters, a correlation between a high PSV and the stabilization potential was demonstrated. This approach is thus transferred to the milling process. Therefore, the surface created in a geometrically idealized cut was analyzed for different feed per tooth configurations and structure depths. The zero level is defined at the structure tips. The maximum possible profile height corresponds to the largest structure depth with $d_s = 100$ µm. The feed direction is indicated by $v_f$. With increasing structure depth, an increase in the profile height can be identified (Fig. 15-B). In the case $f_z = 0.2$ mm, the structure width corresponds to the feed per tooth $f_z$ (Fig. 15-A). An uniform profile is obtained in the direction of $v_f$ since subsequent structure elements follow the cut of the initial structure element. In the case of feed $f_z = 0.24$ mm greater than the structure width, large PSV occur at an angle offset to the feed direction. In orthogonal cutting the PSV in feed direction was always considered. However, this representation is deviated from in the milling process. The relevant interaction volume for force transmission, against the dynamic deflection, is therefore not a constant quantity, but depends on the main component of the oscillation orbit, depending on the process parameters. Typically values for alpha are in a range between $\alpha = 30$-$90°$.

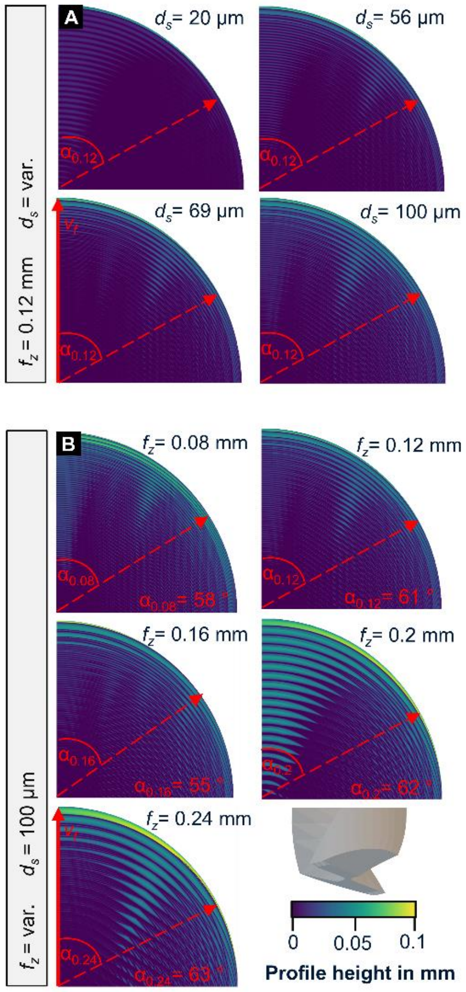


*Fig. 15: Surface structure in dependence of (A) structure depth $d_s$ and (B) feed per tooth $f_z$ configuration.*

Fig. 16 depicted the profile section in the principal direction of oscillation for $f_z = 0.12$ mm. Near the TCP, there is almost no potential for the structural elements to interact with the material due to the low-profile heights and volume. With increasing distance from the TCP, an increase of the profile heights can be noticed. Due to the superimposed translational and rotational motion of the tool, a complex profile is created. In the two-dimensional observation, it could be deduced that there is a dependence of the feed and the structure width $w_s$. Due to the distribution of the PSV towards the circumferential cutting edge, it can be concluded that complete structuring over the entire frontal cutting edge is not necessary or expedient. The accumulated volume in the direction of the principal component axis is compared in Fig. 17 for $N_B = 4$, 10 and 20 structure elements. The structure depth corresponded to the arc radius with $d_s = r_s = 100$ µm. The stabilization volume increased from $V_{PSV} = 0.18$ mm³ at $N_B = 4$ with to a value of $V_{PSV} = 0.26$ mm³ at $N_B = 20$. The difference between 10 (0.25 mm$^3$) and 20 elements (0.26 mm$^3$) is only marginal. A similar stabilization potential can be assumed.

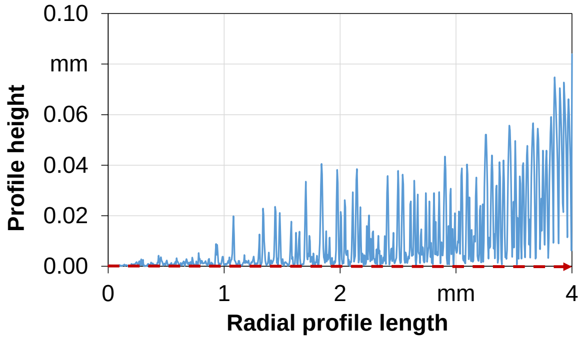


*Fig. 16: Profile height along the main oscillation vector for $d_s$ = 100 µm, $f_z$ = 0.12 mm.*

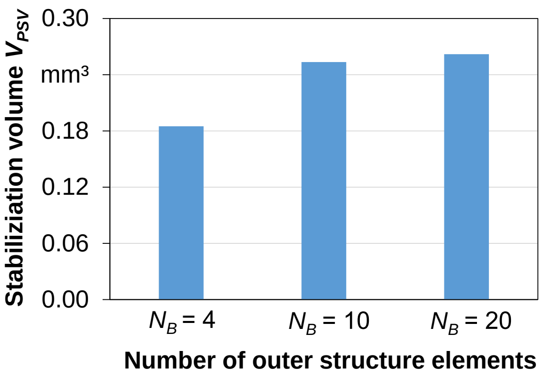


*Fig. 17: Potential stabilization volume depending on the number of outer structure elements.*

## 6 VALIDATION TESTS IN THE MILLING PROCESS

To validate the results of the simulations in the previous chapter, milling experiments were conducted using tools with modified flank face chamfers at the frontal cutting edges.

### 6.1 Test material

The investigations were based on milling tools modified on the frontal cutting edge. The basis was a two-fluted HSS universal milling cutter. The tool diameter was 8 mm with a helix angle of 30°. The tool cantilever length was kept constant at 35 mm, to limit the influence on the dynamic behaviour. The modification of the flank chamfer was performed by micro-milling. A chamfer was applied with a depth of 200 µm, measured from the TCP on the face cutting edge. The chamfer was structured using a ball cutter with diameter $d$ = 200 µm. Three different modifications were produced, all with an arc-shaped structure with a structure width of $w_s$ = 200 µm and $d_s$ = 100 µm. The variation consisted of the number of arc elements applied. Cutter 1 was structured across the entire width of the face cutting edge, cutter 2 was patterned across half of the width, and cutter 3 was structured with only four structure elements (Fig. 18).

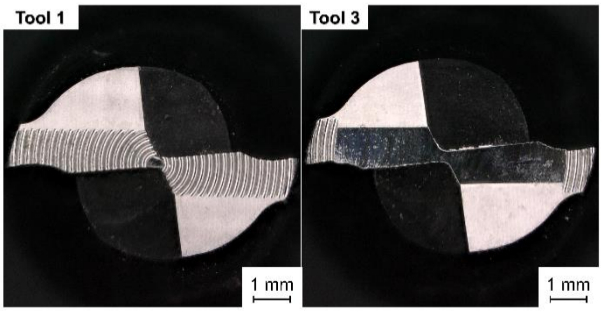


*Fig. 18: Modified milling tool 1 and 3.*

### 6.2 Process design

The machining system was dynamically analyzed (Fig. 19 C) and a specific stability diagram was calculated (Fig. 19 D).

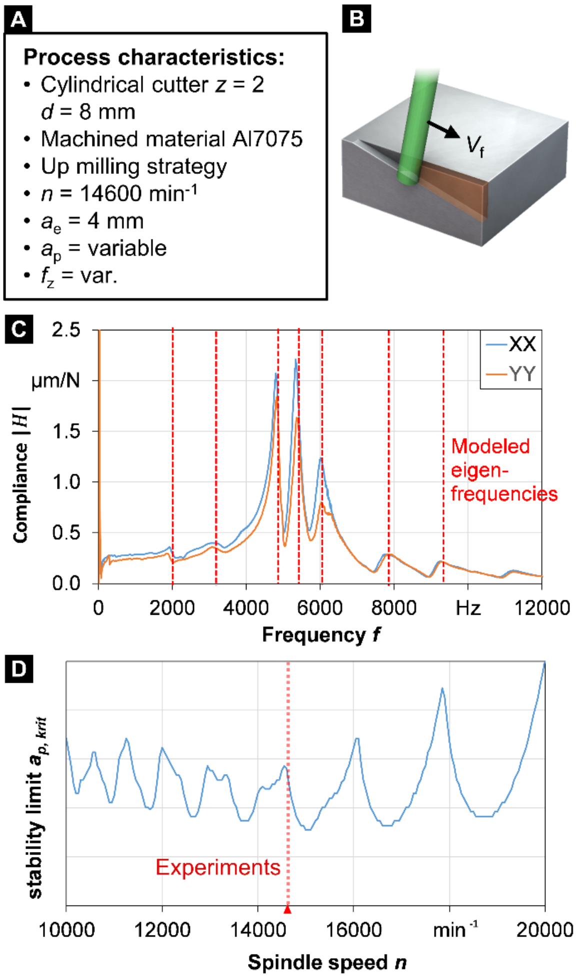


*Fig. 19: Process design and parameter value selection based on simulations.*

The geometric physically-based process simulation [Wiederkehr 2018] was applied with specifically calibrated models of the cutting force and dynamics and typical process parameter values for the investigated application (Fig. 19 A). Based on the stability diagram, a spindle speed of $n$ = 14600 min$^{-1}$ was selected, which comprise a medium high predicted process stability. The selection of the operating point results in a cutting speed of $v_c \approx$ 366 m/min. The prepared tools were experimentally applied in dynamically critical milling processes (Fig. 19 B) with regard to the structure-based modification and spindle speed-specific stability limit. The dynamically critical process is realized by a linear increase of the depth of cut ap, whereby the stability limit is exceeded, and significant dynamic effects start to occur. A constant radial depth of cut of $a_e = 4$ mm and a linearly increasing axial infeed of $a_{p,\,min} = 0$ mm up to $a_{p,\,max} = 11$ mm, which was limited by the length of the cutting edge, were used.

### 6.3 Results

For evaluating the process stability regarding the occurrence of dynamic effects like chatter, face milling processes (Fig. 19-B) were conducted with each structured tool type and the test workpieces were analyzed due to characteristic surface properties like chatter marks. In addition, the acoustic emission during the experiment was evaluated in spectral analysis. The stability limit of the reference tool is compared to the modified tools in Fig. 20. The spindle speed was $n = 14600$ min$^{-1}$ with an radial depth of cut $a_e = 4$ mm and a feed per tooth of $f_z = 0.12$ mm. The axial depth of cut was limited by the length of the peripheral cutter to $a_{p,\,max} = 11$ mm. For the reference tool, the stability limit of $a_{p,\,crit.} = 5.6$ mm can clearly be seen in the onset of chatter oscillations. This limit did not occur for the modified tools, regardless of their number of arc elements.

In the following, the feed per tooth was varied in a range of $f_z = 0.1$-$0.14$ mm. The results show the average values of two tests each with overlayed standard normal deviation (Fig. 21). The reference tool exhibits the lowest stability limit at all feed per tooth rates. The stability minimum occurs at $f_z = 0.1$ mm with $a_{p,\,crit} = 4.7$ mm. The feed per tooth configurations $f_z = 0.12$ and $f_z = 0.14$ mm are equally stable with a value of $a_{p,\,crit} = 5.5$ mm. For the modified milling tools, the stability limit was not reached by any feed per tooth configuration (marked with *). The results are not completely conclusive from a scientific point of view, since the stability limit was not exceeded, and thus the performance of the tool variants could not be evaluated. With a longer cantilevered tool, a lower stability level could be achieved. The simulation showed similar stabilization potential.

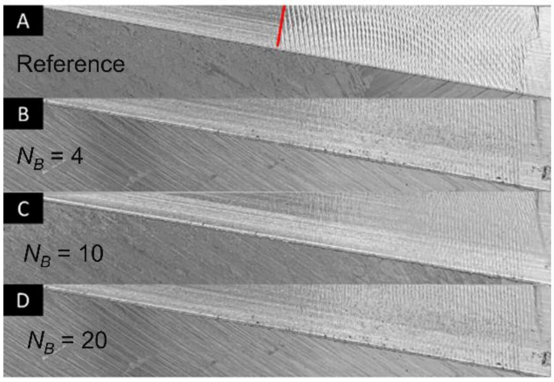


*Fig. 20: Stability limit of Reference tool, and tool variants with different number of structure elements.*

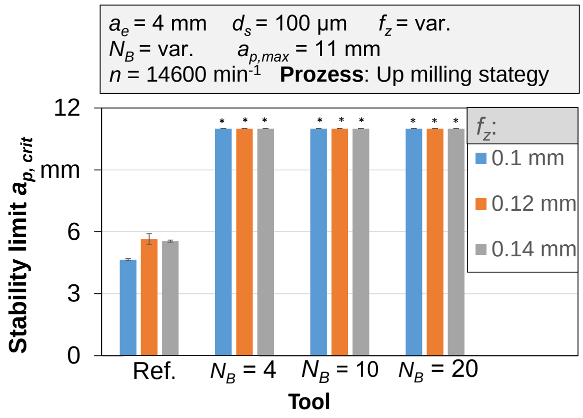


*Fig. 21: Stability limit depending on the tool and the feed per tooth.*

Based on the simulative calculated vibration orbital and the interaction volume as the decisive variable for the stabilization potential, higher feed per tooth values should lead to an increased stabilization potential. However, no statement can be made on this basis of the results. It can be stated that for the process parameters considered, the stabilization potential can be increased by at least 100 % by modifying the flank face on the frontal cutting edges. This applies to tools with $N_B = 4$, 10 and 20 arc elements.

## 7 CONCLUSION

These investigations support the presented working hypothesis on the stabilizing potential of an adapted surface structure on the flank face at the frontal cutting edge of milling tools in the context of process dynamics. The objective was to develop a microstructure-based tool modification and adjusted process configuration that maximizes the stabilization potential. It was deduced that the potential stabilization volume between the workpiece and the structured tool can provide a relevant stabilization potential. Thus, it was verified that arc-shaped structures offer advantages over other structural shapes. With a constant arc radius, semicircular structures showed the greatest potential. This was validated in analogy tests with linear cutting motion in a test environment with dynamically controllable conditions. A correlation between the structure depth and the transmitted tangential force in the direction of the dynamic deflection was determined. The following correlation applies: the greater the structure depth, the greater the transmitted tangential force. An increased normal force with decreasing structure depth could be observed. To increase the analogy of the orthogonal section to the milling process, a feed in tangential direction was introduced, which represented the analogy of the feed per tooth. It could be shown that the transmitting force in the direction of the dynamic deflection, stagnated for all arc depths above a certain number of feed steps. However, since a much more complex vibration orbit is generated in the milling process due to the superimposed rotational and translational motion, compared to the one-dimensional controlled excitation in the analogy experiment, it was first considered geometrically. It was assumed that the PSV in the direction of the main direction of the vibration orbit is decisive for stabilization. The conclusions obtained were used to structure milling tools on the flank face of the frontal cutting edges. It was proven that with the application of an arc-shaped structure, a stabilization potential increased by at least 100 % can be achieved. Influences of the feed per tooth or the number of structure elements on the tool could not be evaluated more precisely, since the stability limit was not reached with any of the modified tool variants. It can be concluded that this work provides important explanatory approaches for evaluating the stabilization potential of microstructures at the flank-surface chamfer of the frontal cutting edge.

## 8 ACKNOWLEDGMENTS

*Gefördert durch die Deutsche Forschungsgemeinschaft (DFG) – Projektnummer 426468684.*

Funded by the German Research Foundation (DFG) – project number 426468684.

## 9 REFERENCES

[Altintas 2014] Altintas, Y.; Kersting, P.; Biermann, D.; Budak, E.; Denkena, B.; Lazoglu, I.: Virtual process systems for part machining operations. CIRP Annals – Manufacturing Technology, 63 (2014) 2, p. 585-605.

[Baumann 2019] Baumann, J., Krebs, E., & Biermann, D.: Chatter avoidance in milling by using advanced cutting tools with structured functional surfaces. MM Sci. J, 4, 3019-3026.

[Denkena 2010] Denkena, B.; de Leon, L.; Grove, T.: Prozessstabilität eines kordelierten Schaftfräsers. Zeitschrift für wirtschaftlichen Fabrikbetrieb, Hanser Verlag, München, 105 (2010), p. 37-41.

[Denkena 2011] Denkena, B.; Tönshoff, H. K.: Spanen – Grundlagen. Springer Verlag, Heidelberg, 2011.

[Denkena 2016] Denkena, B.: Höchste Wirtschaftlichkeit bei der Aluminiumbearbeitung. Maschinenbau – Das schweizer Industriemagazin. 5 (2016), p. 18-22.

[Dietrich 2016] Dietrich, J.: Praxis der Zerspantechnik. Springer Verlag, Vieweg, 2016.

[Hirsch 2012] Hirsch, A.: Werkzeugmaschinen – Grundlagen, Auslegung, Ausführungsbeispiele. Springer Verlag, Vieweg, (2012).

[Möhring 2017] Möhring, H. C.; Wiederkehr, P.; Baumann, J.; König, A.; Spieker, C.; Müller, M.: Intelligent Hybrid Material Slide Component for Machine Tools. Journal of Machine Engineering, (2017) , p. 17-30.

[Munoa 2016] Munoa, J.; Beudaert, X.; Dombovari, Z.; Altintas, Y.; Budak, E.; Brecher, C.; Stepan, G.: Chatter suppression techniques in metal cutting. CIRP Annals - Manufacturing Technology, 65 (2016) 2, p. 785-808.

[Sellmeier 2012] Sellmeier, V.: Über den Einfluss der Werkzeugestalt auf die dynamische Stabilität des Fräsprozesses. Dissertation, Hannover, (2012).

[Vogel 2018] Vogel, F.; Özkaya, E.; Biermann, D.: Additiver Werkzeugaufbau zur Dämpfung von Prozessschwingungen. VDI-Z Integrierte Produktion, 160 (2018) 1/2, p. 42-45.

[Wiederkehr 2018] Wiederkehr, P.; Siebrecht, T.; Baumann, J.; Biermann, D.: Point-based tool representations for modeling complex tool shapes and runout for the simulation of process forces and chatter vibrations. Advances in Manufacturing, Shanghai University und Springer Verlag, (2018).

[Woeste 2021] Wöste, F.; Baumann, J.; Bergmann, J.; Carballo, R. G.; Wiederkehr, P.: Experimental Setup for Analyzing Fundamentals of Cutting Processes using a Modular System. MM Science Journal, (2020) , 3754-3758